Int. J. Electrochem. Sci., 17 **(2022)** Article Number: 221132, doi: 10.20964/2022.11.27

International Journal of
ELECTROCHEMICAL
SCIENCE
www.electrochemsci.org

Synthesis of 3D Co-based Zeolitic Imidazolate Framework and Application as Electrochemical Sensor for H_2O_2 Detection

Zhiqiang Wei, Wei Li, Hui Yang[*]*, Tian Li, Suna He, Yong Wang, Yile Hu*[*]

College of Basic Medical, Henan University of Science and Technology, Luoyang, 471023, Henan, China.
[*]E-mail: yanghui7761@163.com, huyile2@163.com

Received: 8 August 2022 / *Accepted:* 12 September 2022 / *Published:* 10 October 2022

As an emerging hybrid porous coordination polymer comprising organic linkers and metal ions, metal-organic frameworks (MOFs) have shown up excellent electrochemical activity. Co-based zeolitic imidazolate framework (ZIF-67), a novel and special class of MOF with zeolite topological structure, has been deeply studied and employed as electrode materials and catalysis. Of note, ZIF-67 with 3D dodecahedron crystal structure (3D ZIF-67) has became the focus of attention. In this paper, 3D ZIF-67 materials synthesized by two different methods had been contrasted and researched for the first time. The as-prepared materials (3D ZIF-67(H) and 3D ZIF-67(M)) both exhibited typical morphological characteristics and crystal structure of 3D ZIF-67, but there were some slight differences between them. Furtherly, electrochemical sensors for the determination of H_2O_2 were fabricated based on as-prepared materials, and 3D ZIF-67(H) had better hydrophilicity and stability, while 3D ZIF-67(M) had slightly better sensitivity and electrocatalytic activity for the reduction of O_2^{2-}.

Keywords: 3D ZIF-67, Electrochemical Sensing, Synthesis, H_2O_2

1. INTRODUCTION

Metal-organic frameworks (MOFs), the hybrid porous materials comprising organic linkers and metal ions, have been widely employed as gas adsorbents, drug delivery carriers, electrode materials and catalysts due to the unique properties of large specific area, adjustable structure and ordered porosity [1,2]. Zeolite imidazole frameworks (ZIFs), a special MOF subfamily with zeolite topological structure, are tetrahedrally formed by the combination of transition metal ions and imidazolyl ligands, including ZIF-8, ZIF-90, ZIF-L, ZIF-71, ZIF-67, ZIF-7 and so forth [3-6]. ZIF-67 is formed by the reaction of Co^{2+} and imidazole in a suitable solvent, in which imidazole units constitute the bridges connecting Co^{2+} centers [6]. The size and shape of ZIF-67 are easily tuned by adjusting the synthetic conditions, and three typical morphologies of ZIF-67 materials are respectively one-dimensional (1D) nanowires, two-

dimensional (2D) nanosheets, and three-dimensional (3D) rhombic dodecahedron, in which ZIF-67 with 3D dodecahedron crystal structure (3D ZIF-67) has been studied at most [2,7-11]. Methanol is the preferred solvent for the synthesis of 3D ZIF-67, but green synthesis of 3D ZIF-67 using water as solvent has also been reported [2,7-10]. So far, whether there are differences in the characteristics, morphologies and properties of 3D ZIF-67 materials synthesized by different methods has not been studied.

Hydrogen peroxid (H_2O_2) not only acts an important role in chemical industry, food industry and environmental field, but also is deeply related to aging and destructive genetic factors as one of the major reactive oxygen species (ROS) in the human body [7,11,12]. As a key regulator of human biochemical reactions, H_2O_2 in moderation can ensure the normal physiological function and signal transduction of human cells, but excessive or unbalanced H_2O_2 can induce oxidative stress, which leads to organ and tissue damage, even serious human diseases (such aging, Alzheimer's disease, cardiovascular diseases and cancer) [7,11,12]. Therefore, it is of great significance to propose a simple and efficient way for the detection of H_2O_2 in vitro and in vivo. Compared with the conventional methods based spectrometry and colorimetric, electrochemical sensor has became an important mean of H_2O_2 detection because of its advantages, such as good sensitivity, fast response, low-cost and easy miniaturization. In particular, the enzyme-free electrochemical sensor based inorganic nanomaterials seems to be a research hotspot [13-20]. Due to its abundant active sites on the surface, ZIF-67 is fortunately employed to construct the enzyme-free electrochemical sensor for H_2O_2 determination. However, for 3D ZIF-67 materials synthesized by different methods, whether there are some differences as modified materials for electrochemical sensors remains to be furtherly studied.

In the present study, two kinds of 3D ZIF-67 materials were synthesized in methanol and water respectively. Briefly, in the first step we studied and compared the morphologies and crystal structures of these two materials. Then the two materials were employed as electrode modifiers to fabricate nonenzymetic H_2O_2 sensors. Furthermore, based on the fabricated sensors, the electrochemical properties of the two materials were deeply studied. By the comparisons through various physicochemical and electrochemical characterizations, the value and significance of 3D ZIF-67 as an enzyme-free electrochemical sensing material had been further expanded.

2. EXPERMENT

2.1 Reagents

The chemical reagents in this study are all analytical pure and utilized without further refinement. 2-methylimidazole, cobalt nitrate hexahydrate, methanol were obtained from Shanghai Macklin Biochemical Co., Ltd (Shanghai, China). Sulfuric acid, sodium hydroxide, H_2O_2 (30%, w/w) were acquired from Sinopharm Chemical Reagent (Shanghai, China). Nafion (0.5%, w/w) was purchased from Beijing Cool Chemical Technology Co., Ltd (Beijing, China). High-purity water (18.25 MΩ·cm) was prepared by a water purification system (Millipore Direct-Q 3UV，USA), and was utilized in the whole research.

2.2 Apparatus

All electrochemical tests were performed on a electrochemical workstation (CHI 660E, Shanghai Chenhua Instrument Co., Ltd, China), which was equipped with a three-electrode system including a glass carbon electrode (GCE) as the sensor electrode, a platinum wire counter electrode and an Ag/AgCl reference electrode. The drying of 3D ZIF-67 was completed with the aid of vacuum freeze dryer (FD8-3, GOLD SIM Cellular Science LLC, USA). The morphologies of 3D ZIF-67 materials were characterized by scanning electron microscope (JSM-IT 100, JEOL Ltd., Japan). The crystal structures of 3D ZIF-67 materials were evaluated by a powder X-ray diffractometer (D8 Advance, Bruker AXS, Germany).

2.3 Synthesis of 3D ZIF-67

Referring to the previous reports [2，7，21-23], 3D ZIF-67 was synthesized with methanol as the reaction solvent, which was recorded as 3D ZIF-67(M). The specific processes were as follows: 1.940g of cobalt nitrate hexahydrate was dissolved in 200 mL methanol, and 2.178g of 2-methylimidazole was dissolved in another 200 mL methanol. Then, the two separate solutions were mixed and stirred uninterruptedly for 6h at room temperature. Subsequently, the purple precipitates were centrifuged and washed with methanol for six times. Finally, the obtained product was dried for 10h in a vacuum of 100Pa at -20℃.

By changing the reaction solvent and reaction conditions, 3D ZIF-67 synthesized in H_2O solvent was recorded as 3D ZIF-67(H) , and the synthesis processes were as follows: 0.518g of cobalt nitrate hexahydrate was dissolved in 50 mL water, and 5.171g of 2-methylimidazole was dissolved in another 50 mL water. Next, the two separate solutions were mixed and stirred uninterruptedly for 6h at room temperature. Then, the purple precipitates were centrifuged and washed with water for six times. At last, the acquired product was dried for 10h in a vacuum of 100Pa at -20℃.

2.4 Sensor fabrication

Prior to the fabrication, the glass carbon electrode (GCE, 3 mm in diameter) was polished with 50nm alumina slurries for a mirror-like shine, and then ultrasonicated in high-purity water, anhydrous alcohol and high-purity water for 3min respectively [24]. Subsequently, cyclic voltammetry (CV) was carried out in 0.5M H_2SO_4 between -1.0 to +1.0 V for 10 cycles at 0.05V/s to activate the GCE. Finally, the GCE was rinsed with high-purity water, and blown dry with nitrogen for standby.

Afterwards, 20μL of a freshly made dispersion of 3D ZIF-67(M) (1.50mg/mL) was dripped onto the cleaned GCE surface and dried at 25℃. In order to improve the stability of the electrodes, 10 μL nafion solution (0.05%, w/w) was dropped on the surface of modified electrodes. After the modified electrodes were dried, the succedent electrochemical experiments were carried out one after another. 3D ZIF-67(M) modified GCE was recorded as 3D ZIF-67(M)/GCE. For comparing, the same steps were repeated to fabricate 3D ZIF-67(H) modified GCE (3D ZIF-67(H)/GCE).

3. RESULTS and DISCUSSION

3.1 Morphology and Structure Characterizations of 3D ZIF-67(H) and 3D ZIF-67(M)

SEM and XRD were employed to characterize morphologies and crystal structures of the as-synthesized 3D ZIF-67 materials. Figure 1 showed the SEM images of the 3D ZIF-67(M) and 3D ZIF-67(H) respectively. The 3D ZIF-67(M) was typical rhombic dodecahedra with a extraordinary smooth surface, however the 3D ZIF-67(H) had the structural characteristics of rhombic dodecahedron with a slightly rough surface. Compared with 3D ZIF-67(M), the particle size of 3D ZIF-67(H) was a little smaller.

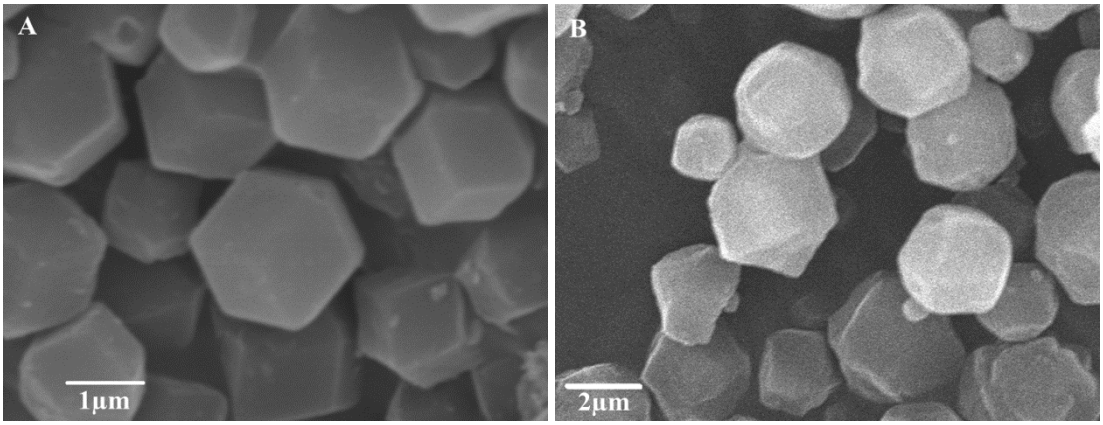

Figure 1. A: SEM image of 3D ZIF-67(M). B: SEM image of 3D ZIF-67(H).

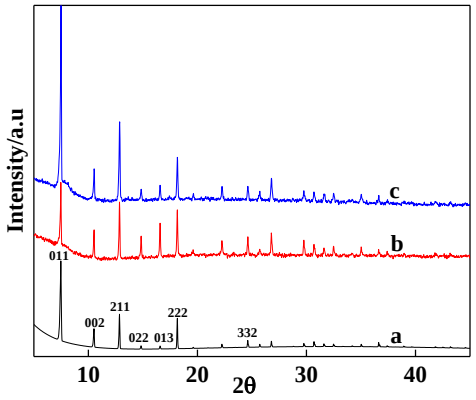

Figure 2. XRD patterns of (a) simulated ZIF-67, (b) 3D ZIF-67(H) and (c) 3D ZIF-67(M).

As shown in Figure 2, for the as-prepared products (3D ZIF-67(H)、3D ZIF-67(M)), the 2θ angles of the XRD diffraction peaks were 7.49°, 10.52°, 12.87°, 14.84°, 16.59° ,18.15° and 24.64°, which were in conformity with (011), (002), (211), (022), (013), (222) and (332) crystal planes of the simulated ZIF-67 (Cambridge Crystallographic Database Centre, CCDC deposition number = 671073), respectively [25-28]. Compared with 3D ZIF-67(H), 3D ZIF-67(M) had stronger intensities of XRD

diffraction peaks, indicating that the crystal structure of 3D ZIF-67(M) was more perfect, which was consistent with SEM images [29]. In conclusion, 3D ZIF-67(M) and 3D ZIF-67(H) had high purity and crystallinity, and were synthesized successfully. The hydration between Co^{2+} and H_2O may inhibit the binding of C_O^{2+} to imidazole ligands, which resulted in the irregular morphology of 3D ZIF-67(H) prepared in aqueous solution.

3.2 Electrochemical study

3.2.1 Cyclic voltammetric responses of 3D ZIF-67(H)/GCE and 3D ZIF-67(M)/GCE

Herein, the electrochemical behaviors of 3D ZIF-67(H) and 3D ZIF-67(M) were studied by cyclic voltammetry (CV). Figure 3 showed cyclic voltammograms obtained at bare GCE , 3D ZIF-67(H)/GCE, 3D ZIF-67(M)/GCE in absence and present of 3.0 mM H_2O_2 solution containing 0.2 M NaOH. When the test solution is in absence of 3.0 mM H_2O_2, each of the three electrodes has a reduction peak: -0.373V at bare GCE, -0.380V at ZIF-67(H)/GCE, -0.417V at 3D ZIF-67(M)/GCE, which correspond to the electrochemical reduction of Co^{3+} [30-32]. The reduction potential of Co^{3+} in 3D ZIF-67(H) was 37mv higher than that in 3D ZIF-67(M), implying that overpotential of 3D ZIF-67(H) is relatively lower, which may be because 3D ZIF-67(H) has better hydrophilicity. Compared with bare GCE, the reduction peak current values at 3D ZIF-67(M)/GCE and 3D ZIF-67(H)/GCE are greatly improved, especially 3D ZIF-67(M)/GCE has better performance, implying that Co^{2+}/Co^{3+} electroactive center in 3D ZIF-67 with a large number of micropores and mesopores improves the conductivity and electrocatalytic performance of GCE [30-32].

With the addition of 3.0 mM H_2O_2 into 0.2 M NaOH solution, each of the three electrodes also had a reduction peak: -0.419V at bare GCE, -0.409V at ZIF-67(H)/GCE, -0.439V at 3D ZIF-67(M)/GCE, which corresponded to the electrochemical reduction of O_2^{2-} [7]. The reduction potential of O_2^{2-} at 3D ZIF-67(M)/GCE was lowest, and the reduction potential of O_2^{2-} at 3D ZIF-67(H)/GCE was highest, implying that 3D ZIF-67(H) and 3D ZIF-67(M) can change the reduction overpotential of O_2^{2-}, which may be caused by the different hydrophilicity of the two materials. For the reduction of O_2^{2-}, the electrocatalytic performances of 3D ZIF-67(M)/GCE and 3D ZIF-67(H)/GCE were significantly better than that of bare GCE, which may be because rich Co^{2+} active centers in 3D ZIF-67 promoted the reduction of H_2O_2 [7]. However the reduction peak current value at 3D ZIF-67(M)/GCE was slightly higher than that at 3D ZIF-67(H)/GCE, which may be because 3D ZIF-67(M) with higher crystallinity had more Co^{2+}/Co^{3+} electroactive centers. Given all of that, 3D ZIF-67(H) had better hydrophilicity, while 3D ZIF-67(M) had better electrocatalytic performance for the reduction of O_2^{2-}. This may be because that the hydration between Co^{2+} and H_2O resulted in inherent hydrophilicity of 3D ZIF-67 (H), and the tight binding of C_O^{2+} with imidazole ligands under anhydrous conditions leaded to more active Co^{2+} ions in 3D ZIF-67(M).

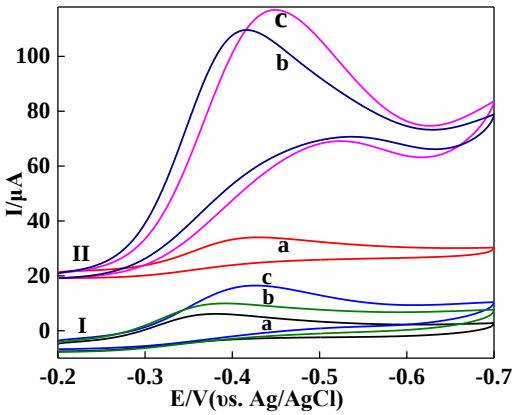

Figure 3. Cyclic voltammograms obtained at (a) bare GCE, (b) 3D ZIF-67(H)/GCE, (c) 3D ZIF-67(M)/GCE in (I) 0.2 M NaOH and (II) 3.0 mM H_2O_2 containing 0.2 M NaOH, scan rate: 0.1 V/s.

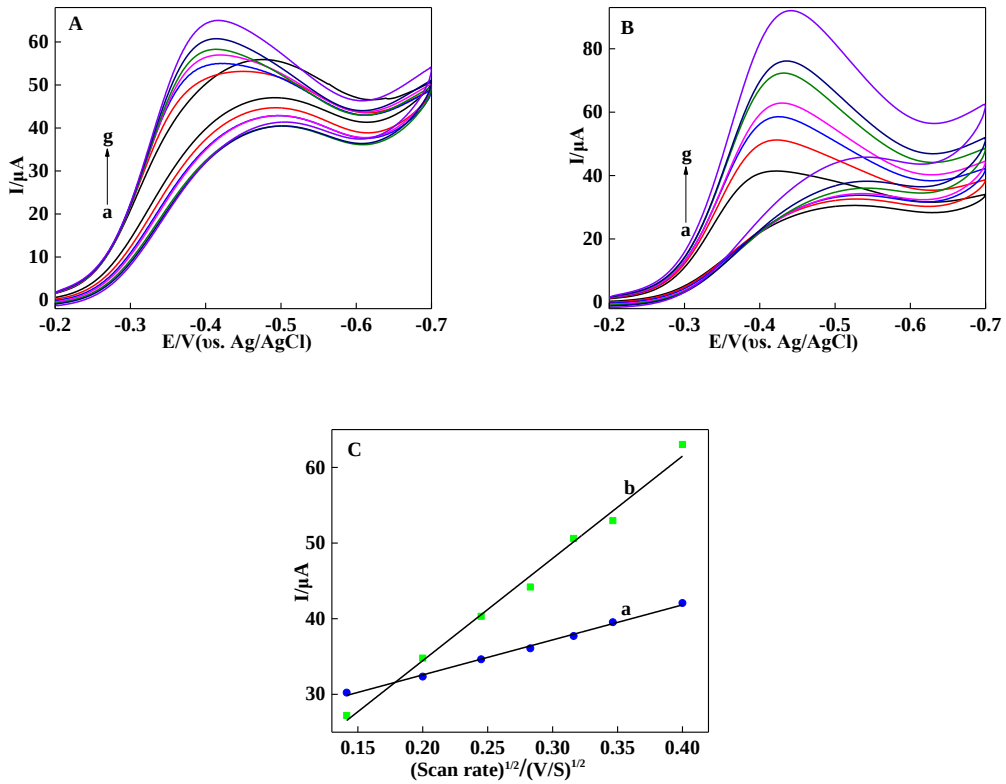

Figure 4. A: Cyclic voltammograms at different scan rates (a-e: 0.01-0.16 V/s) at 3D ZIF-67(H)/GCE in 3.0 mM H_2O_2 containing 0.2 M NaOH . B: Cyclic voltammograms at different scan rates (a-e: 0.01-0.16 V/s) at 3D ZIF-67(M)/GCE in 3.0 mM H_2O_2 containing 0.2 M NaOH. C. Plots of peak current density against the square root of the scan rate at (a) 3D ZIF-67(H)/GCE and (b) 3D ZIF-67(M)/GCE.

In order to further evaluate the effect of scan rate upon the reduction behaviors of O_2^{2-} on 3D ZIF-67(H)/GCE and 3D ZIF-67(M)/GCE, the two electrodes were characterized by CV at different scan

rates (20, 40, 60, 80, 100, 120, 160 mV/s) in 0.2 M NaOH containing 3.0 mM H_2O_2 , as shown in Figure 4. It was easy to find that the peak currents were in good linear with the square root of the scan rates （3D ZIF-67(H)/GCE：Ip (μ A) = 46.271 $v^{1/2}$ + 23.320, R^2 = 0.998; 3D ZIF-67(M)/GCE：Ip (μ A) = 135.147 $v^{1/2}$ + 7.432, R^2 = 0.996). These results indicated that the electrochemical reductions of O_2^{2-} at 3D ZIF-67(H)/GCE and 3D ZIF-67(M)/GCE were controlled by diffusion [33-35].

3.2.2 Amperometric responses of 3D ZIF-67(H)/GCE and 3D ZIF-67(M)/GCE

In order to further survey the electrochemical performances of the two materials, amperometric technology was employed to detect 0.2 mM H_2O_2 in 0.2 M NaOH at different applied potentials (-0.34 V, -0.36 V, -0.38V and -0.40 V). As depicted in Figure 5, the most sensitive and stable current responds of 3D ZIF-67(H)/GCE and 3D ZIF-67(M)/GCE were both occurred at -0.38 V, so we selected -0.38 V as the optimum working potential for further use.

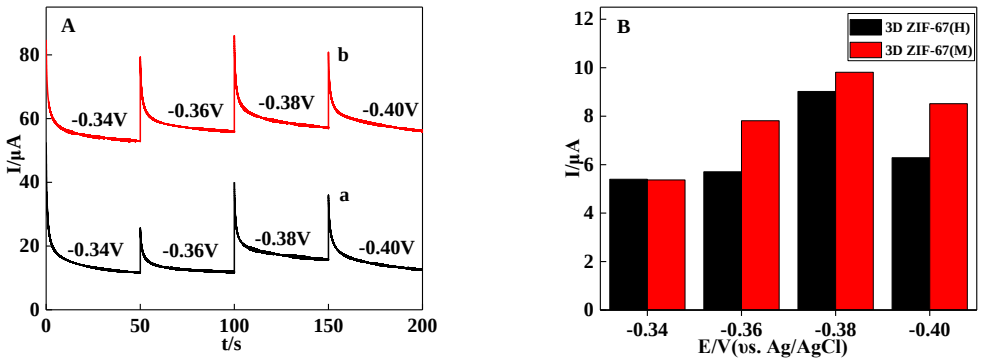

Figure 5. A: Amperometric responses of (a) 3D ZIF-67(H)/GCE and (b) 3D ZIF-67(M)/GCE in 0.2 M NaOH containing 0.2 mM H_2O_2 at different working potentials: -0.34 V, -0.36 V, -0.38 V and -0.40 V. B: Histogram of amperometric current responds vs reduction potentials.

3.2.3 Amperometric measurement of H_2O_2

The sensing performances of 3D ZIF-67(H)/GCE and 3D ZIF-67(M)/GCE were further surveyed by amperometry at -0.38 V. Under the optimized experimental conditions, the amperometric responses pertaining to the increasing concentrations of H_2O_2 were depicted in Figure 6. The current responses of 3D ZIF-67(H)/GCE and 3D ZIF-67(M)/GCE were found to increase with the increase of H_2O_2 concentration. In the low concentration range of H_2O_2 (1 - 35 μM), 3D ZIF-67(M)/GCE had a apparent linear correlation between the current and the H_2O_2 concentration, but there was not obviously linear relation in the current of 3D ZIF-67(H)/GCE and the H_2O_2 concentration. Surprisingly, in the high concentration range of H_2O_2 (30 - 180 μM), 3D ZIF-67(H)/GCE exhibited a good linear dependence of I (μA) on Concentration (μM), which was not available in ZIF-67(M)/GCE. The linear equations were as follows:

I (μA) = 0.1352 c (μM) + 2.5757 (3D ZIF-67(M)/GCE, R^2 = 0.9971， 1 to 35 μM);

I (μA) = 0.0055 c (μM) + 7.1923 (3D ZIF-67(H)/GCE, R^2 = 0.9991， 30 to 180 μM).

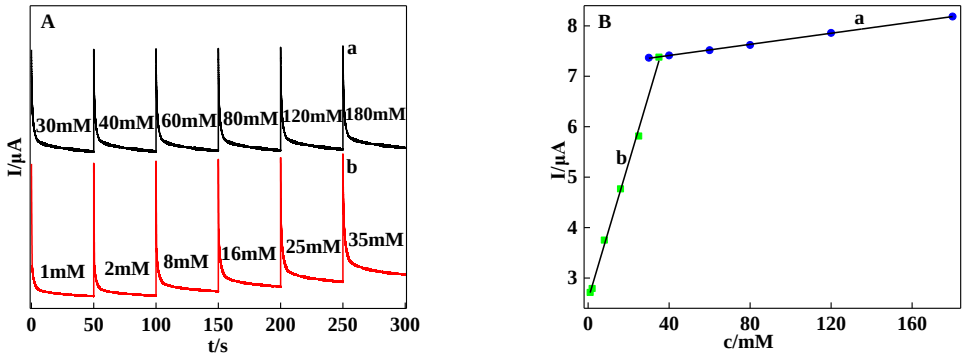

Figure 6. A: Amperometric responses obtained at (a) 3D ZIF-67(H)/GCE and (b) 3D ZIF-67(M)/GCE in 0.2M NaOH containing different concentrations of H_2O_2. B: The linear relationship of amperometric current and the concentration of H_2O_2 ((a) 3D ZIF-67(H)/GCE: 30- 180 μM, (b) 3D ZIF-67(M)/GCE: 1- 35 μM). Applied potential: -0.38 V.

The comparison of analytical performance between present work and earlier reports was given in Table 1. The data showed that 3D ZIF-67(M)/GCE had superior analytical performance for the determination of low concentration H_2O_2. 3D ZIF-67(M) and 3D ZIF-67(H) can be used in pairs as electrode modification material for determination of H_2O_2, which can realize low detection limit and wide detection range.

Table 1. List of various electrodes reported in literature for determination of H_2O_2

Electrode	Linear range (μM)	Ref.
Co_3O_4/MWCNTs/CPE	20-430	[30]
Nafion/GOD-NanoCoPc-Gr/ GCE	10-600	[36]
MIL-53-Cr^{III}_{AS}/GCE	25-500	[37]
Co_3O_4-NWs/CF	10-1400	[38]
Fe-MOF/rGO/CPE	5-945	[39]
3D ZIF-67(M)/GCE	1-35	This work
3D ZIF-67(H)/GCE	30-180	

4. CONCLUSIONS

For the first time, a comparative study of 3D ZIF-67 materials synthesized by two different ways (3D ZIF-67(H) and 3D ZIF-67(M)) was made. 3D ZIF-67(H) and 3D ZIF-67(M) both exhibited the typical characteristics of 3D ZIF-67, but 3D ZIF-67(M) had smoother surface and higher crystallinity. Electrochemical sensors based on 3D ZIF-67(M) (3D ZIF-67(M)/GCE) illustrated better sensitivity and low concentration detection linearity, while electrochemical sensors based on 3D ZIF-67(H) (3D ZIF-67(H)/GCE) showed better hydrophilicity and high concentration detection linearity for the reduction

of O_2^{2-}. In summary, this work is instructive to promote the application of 3D ZIF-67 in the field of electrochemical sensors.

ACKNOWLEDGEMENTS
This work was supported by the Key Project of Science and Technology of Henan (Grant No.2021023 10488).

References

1. X.R. Chen, D. Lau, G.J. Cao, Y. Tang, and C. Wu, *ACS Appl. Mater. Interfaces*, 11(2019) 9374.
2. D.P. Sun, D.C. Yang, P. Wei, B. Liu, Z.G. Chen, L.Y. Zhang, and J. Lu, *ACS Appl. Mater. Interfaces*, 12(2020) 41960.
3. P.H. Tong, J.Y. Liang, X.X. Jiang and J.P. Li, *Crit. Rev. Anal. Chem*., 50(2020) 376.
4. P. Kukkar, K.H. Kim, D. Kukkar and P. Singh, *Coord. Chem. Rev*., 446 (2021), doi: 10.1016/j.ccr.2021.214109.
5. Y.V. Kaneti, S. Dutta, M.S.A. Hossain, M.J.A. Shiddiky, K.L. Tung, F.K. Shieh, C.K. Tsung, K.C.W. Wu and Y. Yamauchi, *Adv. Mater*., 29(2017), doi: 10.1002/adma.201700213.
6. J. Zhang, Y. Tan and W.J. Song, *Microchim*. Acta, 187(2020), doi: 10.1007/s00604-020-4173-3.
7. Y.H. Dong and J.B. Zheng, *Chem. Eng. J*., 392(2020), doi: 10.1016/j.cej.2019.123690.
8. F. Hashemi, A.R. Zanganeh, F. Naeimi and M. Tayebani, *Anal. Bioanal. Chem*., 413(2021) 5215.
9. N.S. Lopa, M.M. Rahman, F. Ahmed, T. Ryu, J. Lei, I. Choi, D.H. Kim, Y.H. Lee and W. Kim, *J. Electroanal. Chem*., 840(2019) 263.
10. E. Sohouli, M.S. Karimi, E.M. Khosrowshahi, M. Rahimi-Nasrabadi and F. Ahmadi, Measurement, 165(2020), doi: 10.1016/j.measurement.2020.108140.
11. Y.H. Dong and J.B. Zheng, *Sens. Actuators, B*, 311(2020), doi: 10.1016/j.snb.2020.127918.
12. H.F. Wang, W.X. Chen, Q.Y. Chen, N. Liu, H.J. Cheng and T. Li, *J. Electroanal. Chem*., 897(2021), doi: 10.1016/j.jelechem.2021.115603.
13. O. Seven, F. Sozmen and I.S. Turan, *Sens. Actuators, B*, 239(2017) 1318.
14. L. Sun, Y. Ding, Y. Jiang and Q. Liu, *Sens. Actuators, B*, 239(2017) 848.
15. C.J. Gao, H.M. Zhu, J. Chen and H.D. Qiu, *Chin. Chem. Lett*., 28(2017) 1006.
16. M.R. Song, J.L. Wang, B.Y. Chen and L. Wang, *Anal. Chem*., 89(2017) 11537.
17. A.T.E. Vilian, S.M. Chen and B.S. Lou, *Biosens. Bioelectron*., 61(2014) 639.
18. A.A. Ensafi, F. Rezalo and B. RezaeiDepartment, *Sens. Actuators, B*, 231(2016) 239.
19. S.J. Tong, Z.Z. Li, B.L. Qiu, Y.N. Zhao and Z.H. Zhang, *Sens. Actuators, B*, 258(2018) 789.
20. M. Thiruppathi, P.Y. Lin, Y.T. Chou, H.Y. Ho, L.C. Wu and J.A.A. Ho, *Talanta,* 200(2019) 450.
21. G.J. Wei, Z. Zhou, X.X. Zhao, W.Q. Zhang and C.H. An, *ACS Appl. Mater. Interfaces*, 10(2018) 23721.
22. H.B. Zhang, Z.J. Ma, J.J. Duan, H.M. Liu, G.G. Liu, T. Wang, K. Chang, M. Li, L. Shi, X.G. Meng, K.C. Wu and J.H. Ye, *ACS Nano*, 10(2016) 684.
23. Y.H. Dong, C.Q. Duan, Q.L. Sheng and J.B. Zheng, *Analyst (Cambridge, U. K.),* 144(2019) 521.
24. M.X. Zhang, M.S. Li, W.G. Wu, J.K. Chen, X.L. Ma, Z.J. Zhang and S.C. Xiang, *New J. Chem*., 43(2019) 3913.
25. Y.Q. Tian, C.X. Cai, X.M. Ren, C.Y. Duan, Y. Xu, S. Gao, and X.Z. You, *Chemistry*, 9(2003) 5673.
26. S.A. Ahmed, D. Bagchi, H.A. Katouah, M.N. Hasan, H.M. Altass and S.K. Pal, *Sci. Rep.*, 9(2019) , doi: 10.1038/s41598-019-55542-8.
27. R. Banerjee, A. Phan, B. Wang, C. Knobler, H. Furukawa, M. O'Keeffe and O.M. Yaghi, *Science (Washington, DC, U. S.)*, 319(2008) 939.

28. Z. Jiang, Z. Li, Z. Qin, H. Sun, X. Jiao and D. Chen, *Nanoscale*, 5 (2013)11770.
29. N.S. Lopa, M.M. Rahman, F. Ahmed, T. Ryu, J. Lei, I. Choi, D.H. Kim, Y.H. Lee and W. Kim, *J. Electroanal. Chem.,* 840(2019) 263.
30. H. Heli and J. Pishahang, *Electrochim. Acta*, 123(2014) 518.
31. L.Yang, C. Xu, W. Ye and W. Liu, *Sens. Actuators, B*, 215 (2015) 489.
32. L.L. Xiao, Q. Zhao, L. Jia, Q. Chen, J. Jiang and Q.Y. Yu, *Electrochim. Acta*, 304 (2019) 456.
33. H. R. Zare, B. Moradiyan, Z. Shekari and A. Benvidi, *Measurement*, 90(2016) 510.
34. Z.Q. Wei, Y.L. Hu, Q.Q. Tu, S.M. Cui, Y.R. Li, Y. Gan, G.L. Li, H. Yang and S.Q. Li, *Int. J. Electrochem. Sci.,* 12 (2021), doi: 10.20964/2021.06.23.
35. H. Yang, Z.Q. Wei, S.N. He, T. Li, Y.F. Zhu, L.X. Duan, Y. Li and J.G. Wang, *Int. J. Electrochem. Sci.*, 12 (2017) 11089.
36. H.H. Wang, Y. Bu, W.L. Dai, K. Li, H.D. Wang and X. Zuo. *Sens. Actuators, B*, 216 (2015) 298.
37. N.S. Lopa, M.M. Rahman , F. Ahmed, S.C. Sutradhar, T. Ryu and W. Kim. *Electrochim. Acta*, 274 (2018) 49.
38. M.M. Liu, S.J. He and W. Chen, *Nanoscale*, 6 (2014) 11769.
39. S.L. Yang, M.Y. Li, Z.L. Guo, N. Xia and L.B. Qu. *Int. J. Electrochem. Sci*, 14 (2019) 7703.

© 2022 The Authors. Published by ESG (www.electrochemsci.org). This article is an open access article distributed under the terms and conditions of the Creative Commons Attribution license (http://creativecommons.org/licenses/by/4.0/).